

# Crossed-beams and theoretical study of the reaction dynamics of $O(^3P)$ with cyanoacetylene and acrylonitrile

G. Pannacci,<sup>1</sup> P. Liang,<sup>1</sup> G. Vanuzzo,<sup>1</sup> D. Marchione,<sup>1</sup> P. Recio,<sup>1</sup> P. Casavecchia,<sup>1</sup> F. Ferlin,<sup>1</sup> L. Vaccaro,<sup>1</sup> L. Mancini,<sup>1</sup> E. V. F. de Aragão,<sup>2</sup> M. Rosi,<sup>3</sup> N. Fagnas-Lago<sup>1</sup> and N. Balucani<sup>1</sup>

<sup>1</sup>Dipartimento di Chimica, Biologia e Biotecnologie, Università degli Studi di Perugia, 06123 Perugia, Italy

<sup>2</sup>Master-TEC s.r.l., 06128 Perugia, Italy

<sup>3</sup>Dipartimento di Ingegneria Civile e Ambientale, Università degli Studi di Perugia, 06125 Perugia, Italy

## Introduction:

Nitrogen oxides  $NO_x$  represent a concrete risk to human health and have become a matter of concern for their environmental effects, such as acid rains, photochemical smog, and the accumulation of ground-level ozone.<sup>1</sup> In order to rationalize the total concentration of  $NO_x$  in the atmosphere, predict their evolution, and limit their emission, combustion is one of the most important process that should be taken into account, in addition to natural and biogenic sources.<sup>2,3</sup> In fact, coal and coal-derived liquids contain organonitrogen in pyrrolic and pyridinic functional groups: their thermal decomposition generates many nitrogen-bearing compounds that can undergo subsequent oxidation to  $NO_x$ .<sup>4</sup>

To fully understand these processes, accurate and detailed combustion models are needed, where all elementary chemical steps, their primary products, and channel specific rate constants as a function of temperature and pressure are included. In this context, we have investigated the dynamics of two important elementary reactions:  $O(^3P)$  + cyanoacetylene (CHCCN) and  $O(^3P)$  + acrylonitrile ( $CH_2CHCN$ ). In fact, although it has been assumed in some models that the main precursors of  $NO_x$  are HCN and  $NH_3$ ,<sup>5</sup> the pyrolysis of both heterocyclic compounds, such as pyridine, pyrimidine,<sup>6</sup> 2-picoline (the nitrogen analogue of toluene),<sup>7</sup> and pyrrole,<sup>8</sup> and nitriles, such as acetonitrile,<sup>9</sup> is characterized by a distribution of products, including CHCCN and  $CH_2CHCN$ .

The crossed-molecular-beam (CMB) technique in its "universal" arrangement with mass spectrometric (MS) detection represents an efficient experimental tool to investigate polyatomic multichannel elementary reactions, being particularly suitable to unambiguously identify the primary reaction products with their branching fractions (BFs), and the role of intersystem crossing (ISC).<sup>10</sup> The experimental results are always discussed in the light of dedicated electronic structure calculations of the underlying triplet and singlet potential energy surfaces (PESs).

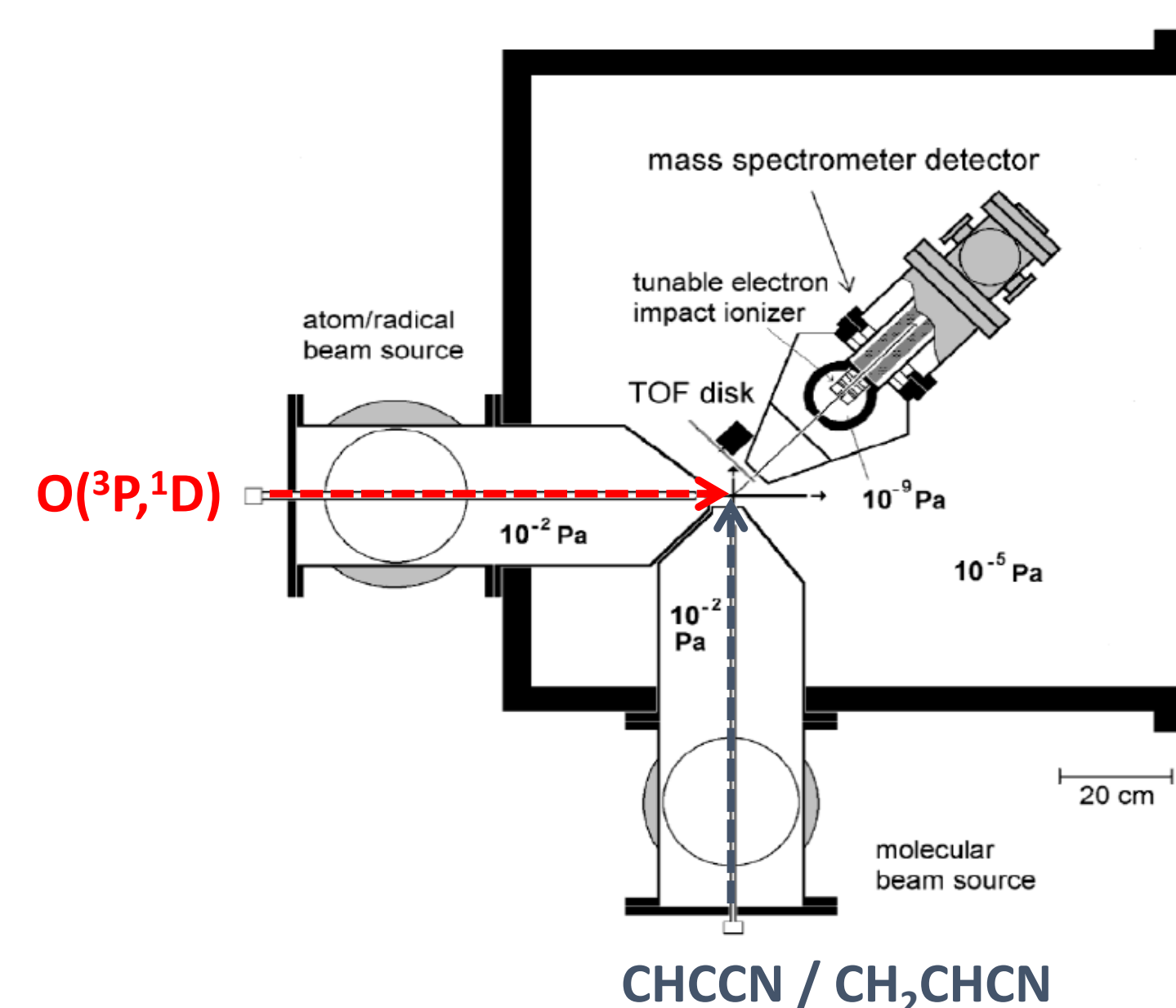
The comparison between the experimental BFs and the theoretical estimates of the relative yields, still underway, will permit to validate the PESs in such a way that accurate and reliable parameters for improved combustion models can be derived.

## Theory:

Regarding the PESs, the geometries of the stationary points were optimized using density functional theory (DFT), with the Becke-3-parameter exchange and Lee-Yang-Parr correlation (B3LYP) functional; the energies of the optimized geometries were computed at coupled-cluster level, including single and double excitations and a perturbative estimate of connected triples (CCSD(T)). Both methods were used in conjunction with the correlation consistent valence polarized basis set aug-cc-pVTZ.

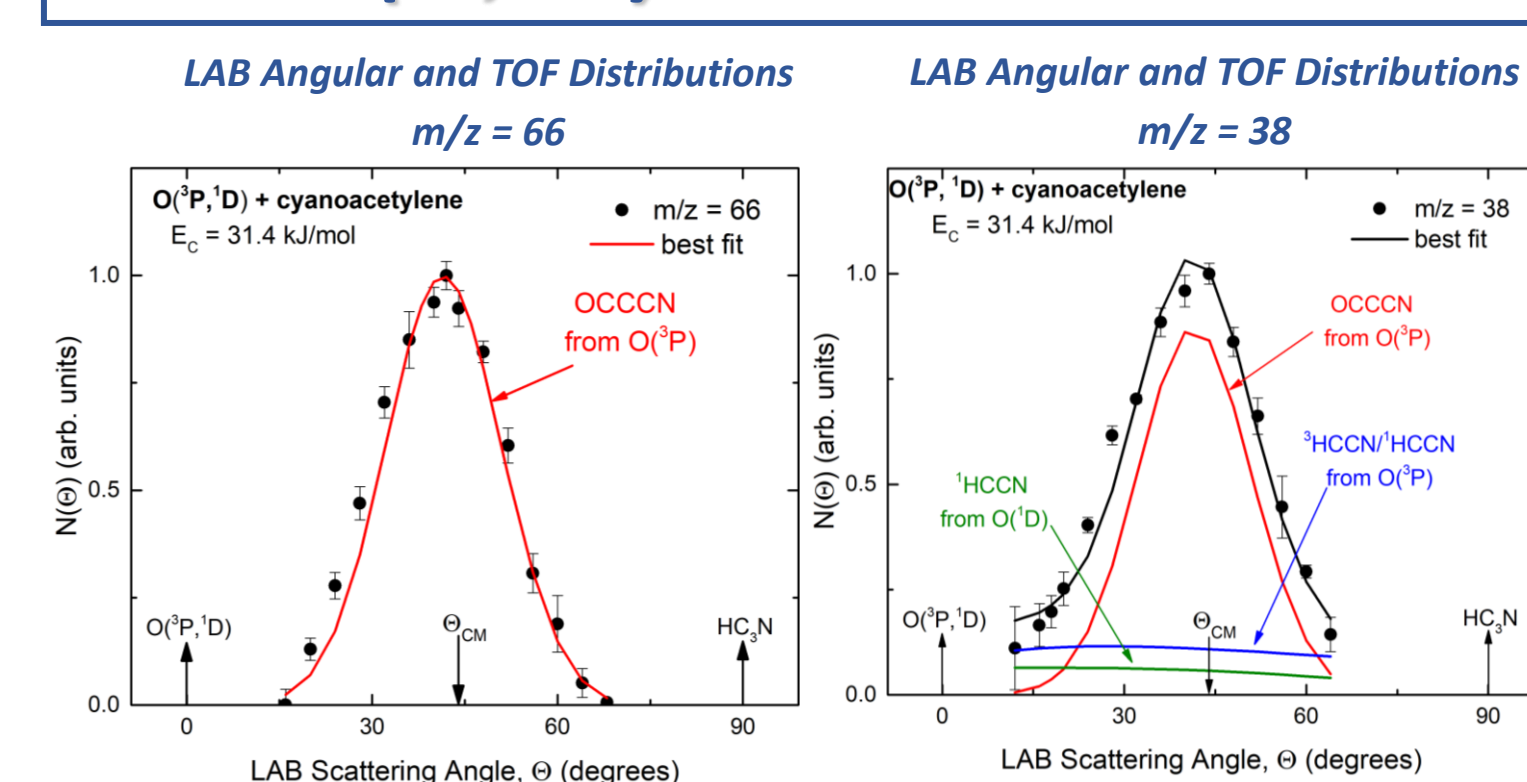
## Experiment:

We have investigated the dynamics of the  $O(^3P)$  + cyanoacetylene and  $O(^3P)$  + acrylonitrile reactions by the crossed molecular beam method at the collision energy,  $E_c$ , of 31.4 kJ/mol and 31.8 kJ/mol, respectively. From product angular and velocity distribution measurements in the LAB frame at different  $m/z$  ratios we have identified the primary product channels, derived the product angular and translational energy distributions in the center-of-mass frame (CM), and determined the branching fractions (BFs). A schematic view of the Perugia crossed molecular beam apparatus is shown below.<sup>11</sup>

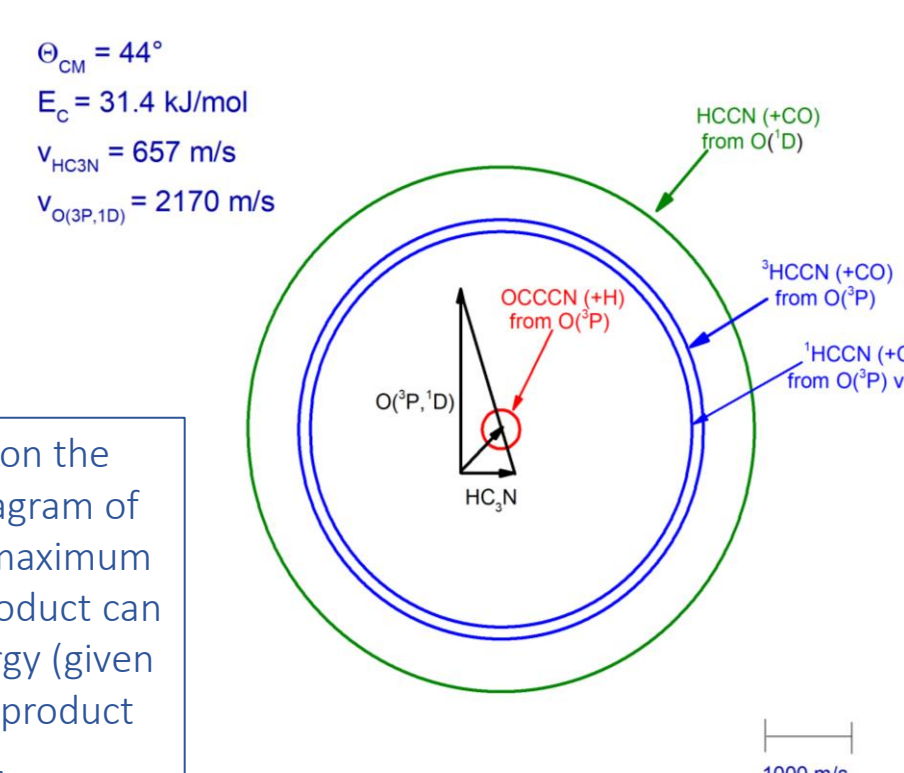


- ✓ Continuous supersonic beams of reactants, crossing angle  $90^\circ$
- ✓ RF discharge source for atomic oxygen beam
- ✓ Rotating mass spectrometer (MS) detector with tunable electron impact ionizer
- ✓ TOF pseudo-random disk for time-of-flight analysis

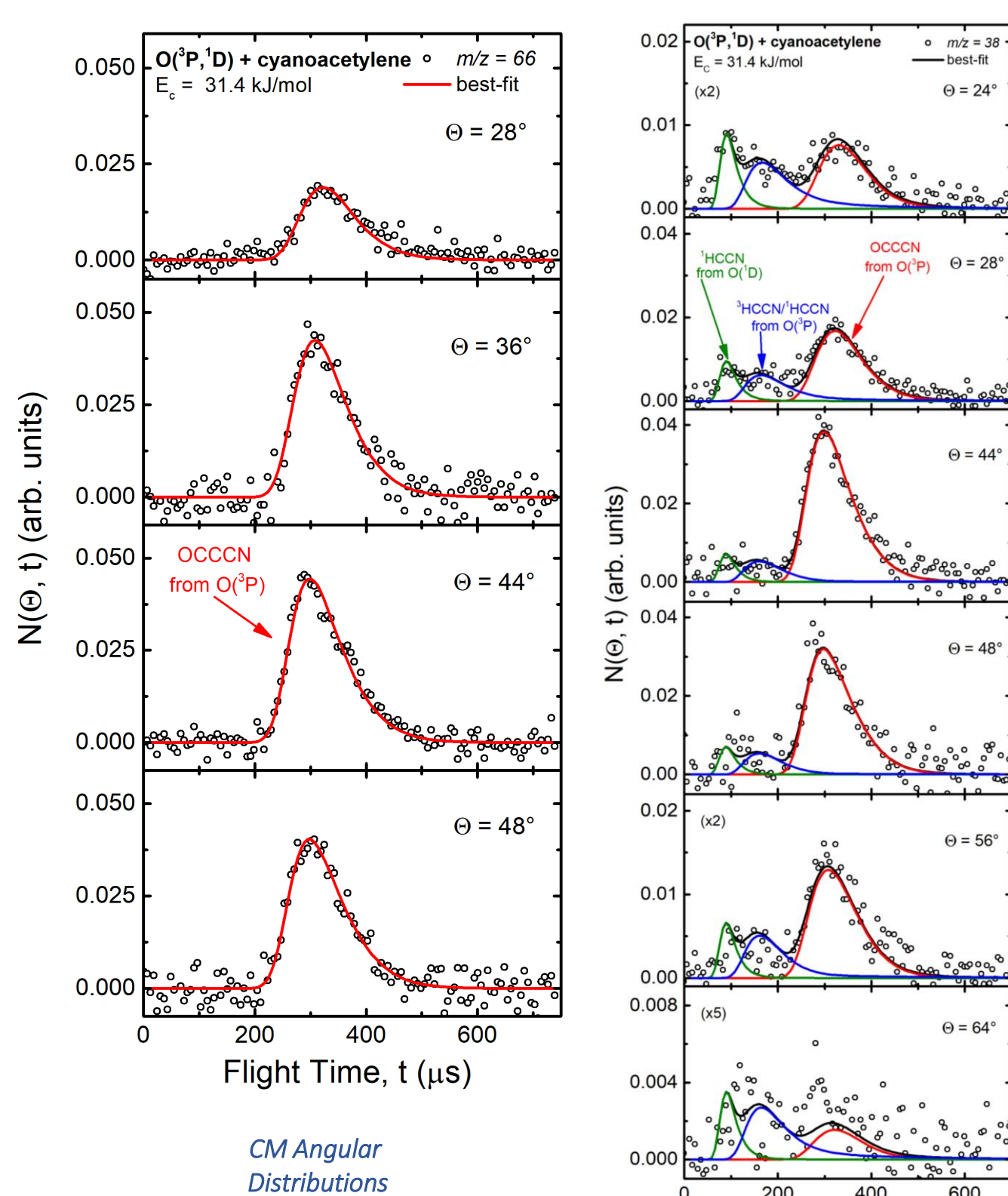
## The $O(^3P, ^1D)$ + CHCCN reaction



### NEWTON DIAGRAM



The circles superimposed on the velocity vector (Newton) diagram of the experiment delimit the maximum velocity that the indicated product can attain if all the available energy (given by  $E_c - \Delta H$ ) is channeled into product translational energy.



### Product channels of the $O(^3P, ^1D)$ + cyanoacetylene reaction:

$m/z = 66$  Signal at this mass originates from the H-displacement channel:  
 $O(^3P) + CHCCN \rightarrow OCCCN + H$

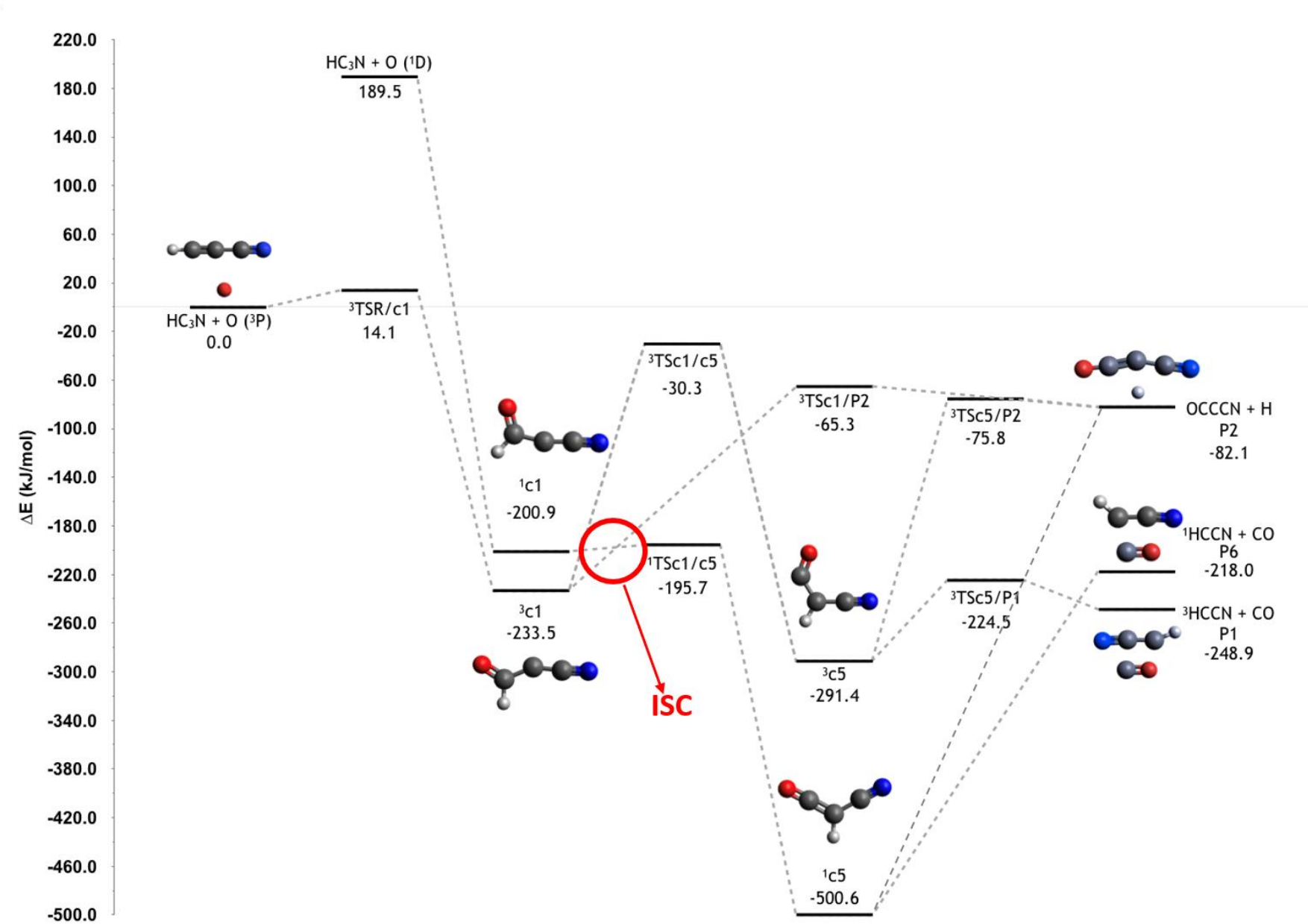
- $m/z = 38$  Signal at this mass can originate from the following different sources:
- fragmentation of OCCCN (from the H-displacement channel on the triplet PES)
  - fragmentation of  $^3HCCN$  or  $^1HCCN$  product from the reaction  $O(^3P) + CHCCN$  occurring adiabatically on the triplet PES, or non-adiabatically (via ISC) on the singlet PES, respectively, and forming  $^3HCCN/^1HCCN + CO$
  - fragmentation of  $^1HCCN$  from the  $O(^1D)$  reaction giving  $^1HCCN + CO$

### Product CM angular and translational energy distributions:

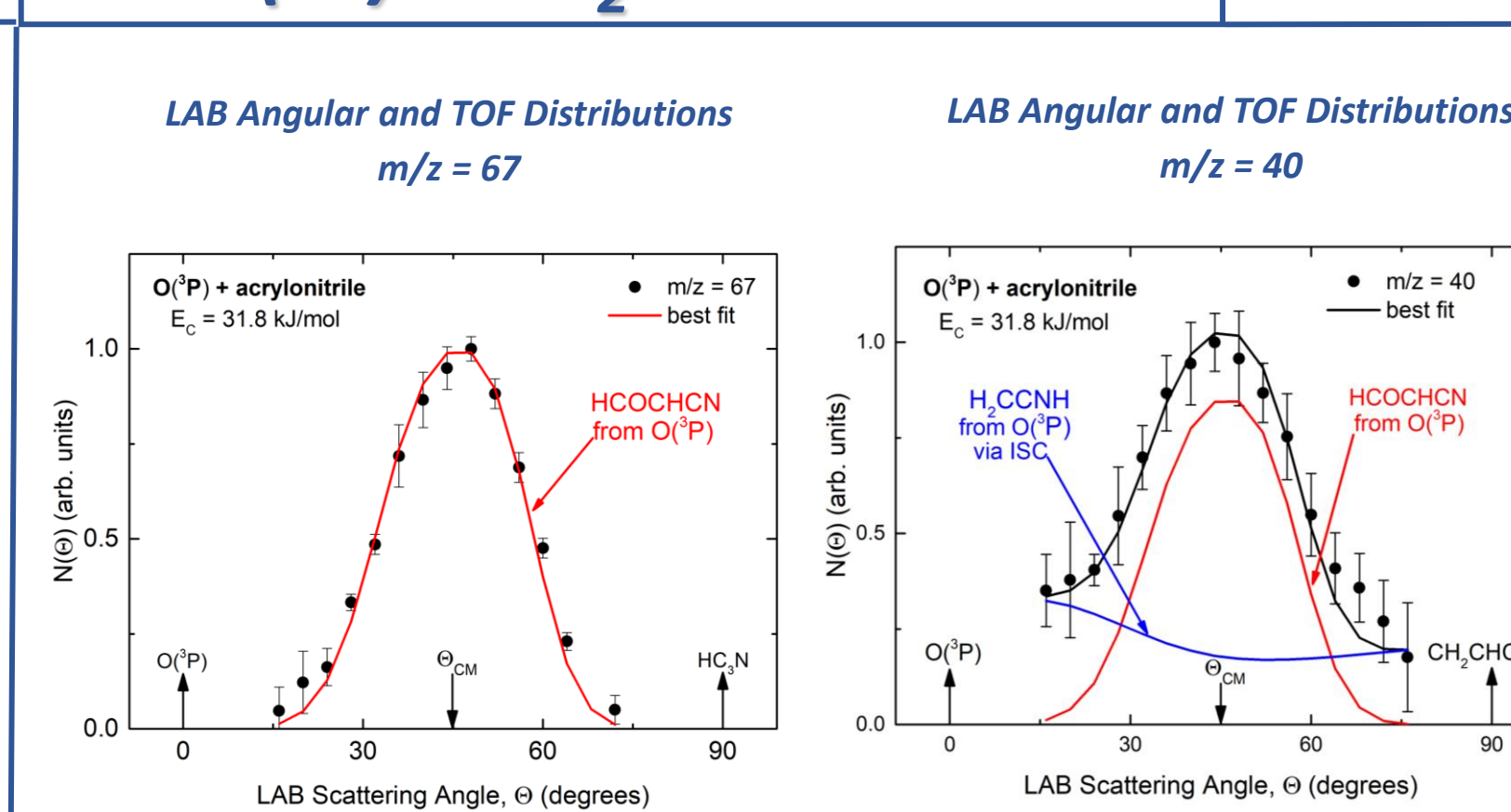
- Formation of OCCCN + H and  $^3HCCN/^1HCCN + CO$  from the  $O(^3P)$  reaction and of  $^1HCCN + CO$  from the  $O(^1D)$  reaction occurs via an oscillating complex, with an asymmetric angular distribution exhibiting a preferential peak in the forward direction.
- Presence of an exit potential energy barrier and available energy essentially channeled into internal excitation in the case of OCCCN and HCCN product from the reaction of  $O(^3P)$ .
- Large fraction of energy channeled into translation in the case of  $^1HCCN$  product from the reaction of  $O(^1D)$  due to the high energy content of  $O(^1D)$ .

Triplet and singlet potential energy surfaces support these considerations.

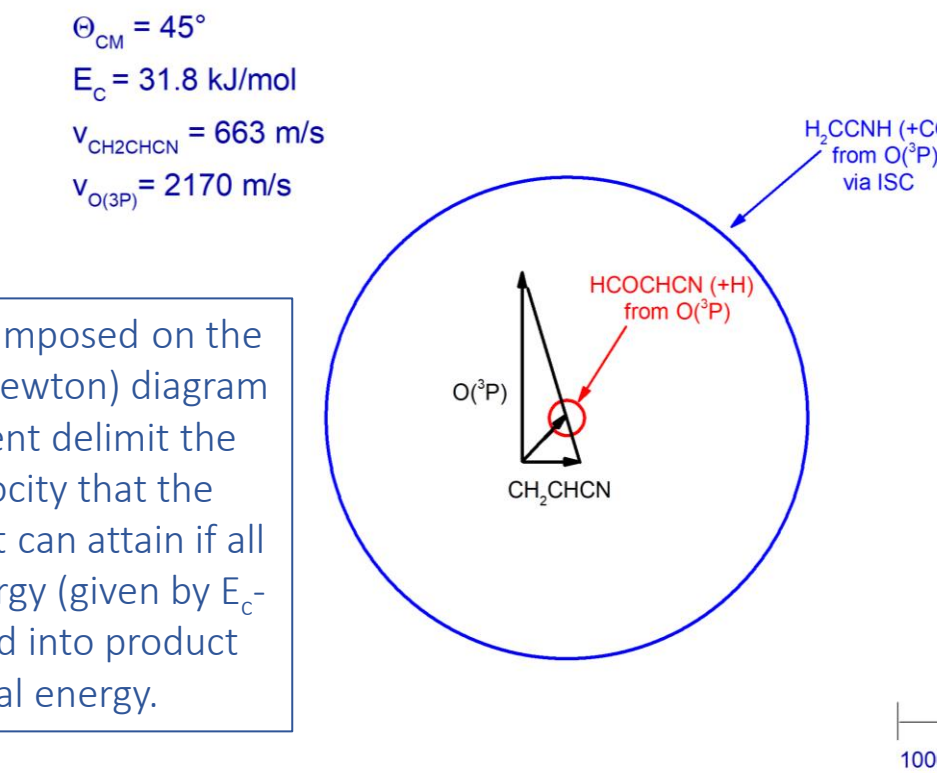
### Simplified PES



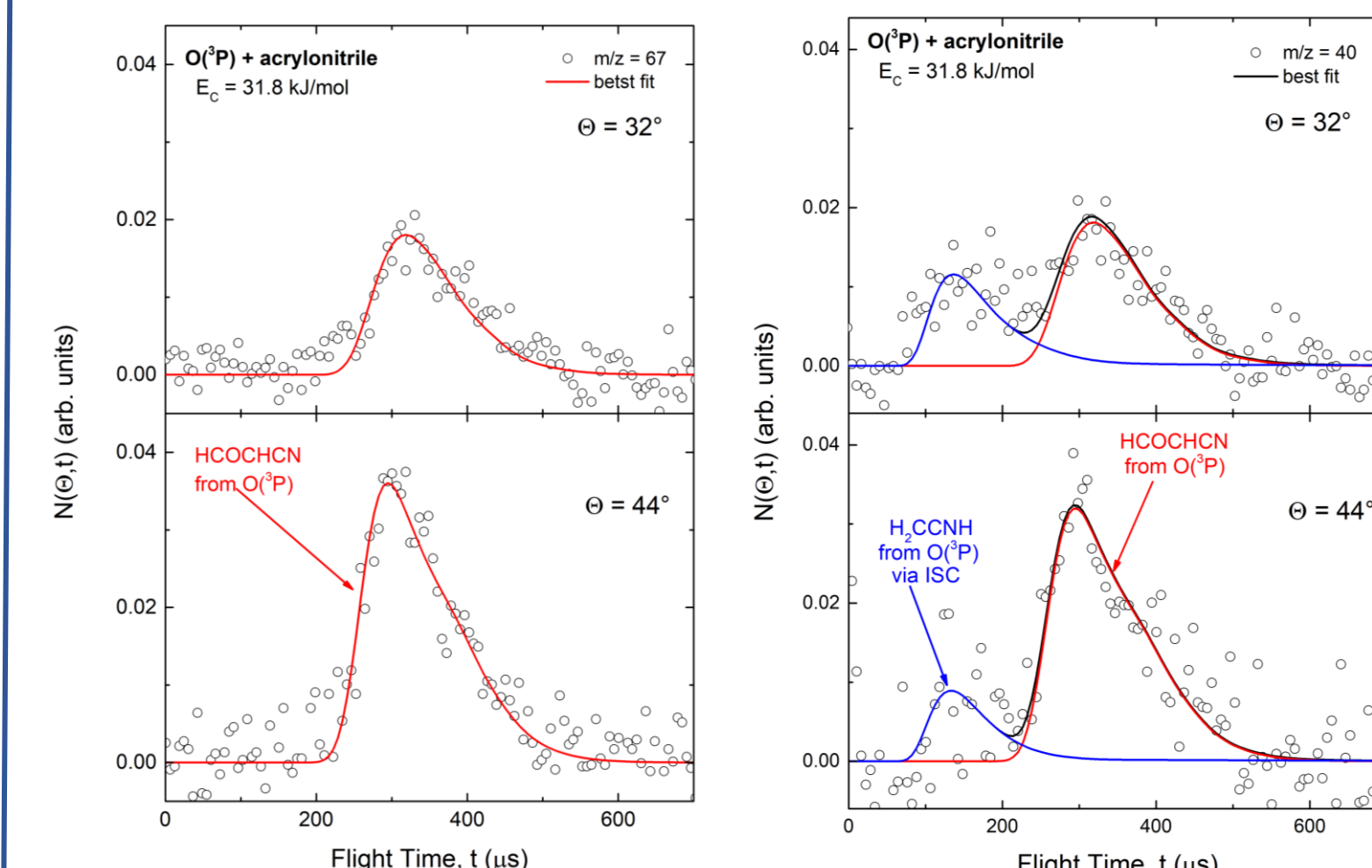
## The $O(^3P)$ + $CH_2CHCN$ reaction



### NEWTON DIAGRAM



The circles superimposed on the velocity vector (Newton) diagram of the experiment delimit the maximum velocity that the indicated product can attain if all the available energy (given by  $E_c - \Delta H$ ) is channeled into product translational energy.



### Product channels of the $O(^3P)$ + acrylonitrile reaction:

$m/z = 67$  Signal at this mass originates from:  
a) fragmentation of HCOCHCN from the HCOCHCN + H product channel

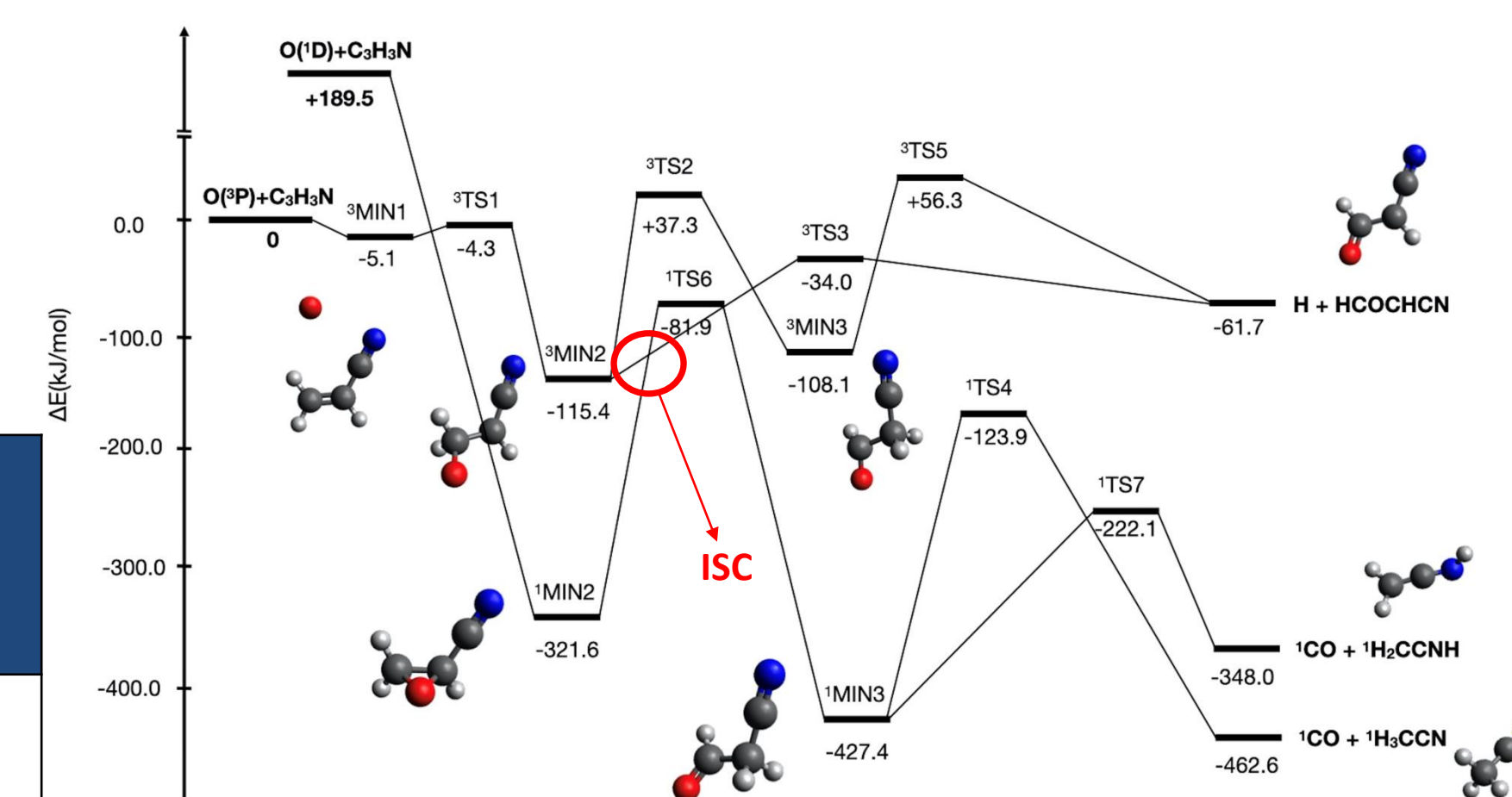
- $m/z = 40$  Signal at this mass can originate from the following different sources:
- fragmentation of HCOCHCN (from the H-displacement channel)
  - fragmentation of  $H_2CCNH$  (ketene imine) from the product channel  $H_2CCNH + CO$  via ISC

### Product CM angular and translational energy distributions:

- Formation of HCOCHCN + H and  $H_2CCNH + CO$  from the  $O(^3P)$  reaction occurs via a long-lived complex, with an isotropic and backward-forward symmetric angular distribution, respectively.
- Presence of an exit potential energy barrier in both cases.

Triplet and singlet potential energy surfaces support these considerations.

### Simplified PES



## $O(^3P)$ + $CH_2CHCN$ reaction

PRIMARY PRODUCTS	$\Delta H^0_0$ (kJ/mol)	B.F.
H + HCOCHCN on triplet PES	-61.7	0.09
CO + $H_2CCNH$ via ISC on singlet PES	-348.0	0.91

Uncertainties on BFs are of about  $\pm 30-50\%$

The experimental branching fractions were calculated following the procedure outlined by Schmoltner et al.<sup>12</sup>

Note that the singlet PES shows the presence of also a more exothermic channel that leads to a constitutional isomer of ketene imine:  $CH_2CN$  (acetonitrile) + CO. We can assert with reasonable certainty that the main channel is  $H_2CCNH + CO$  because this pathway has a lower potential barrier and we had no signal at  $m/z = 41$  (the base peak in the NIST mass spectrum of  $CH_2CN$ ).

## Conclusions:

This work shows that the combined effort of crossed molecular beam experiments and theoretical calculations allows us to understand and interpret the reaction dynamics at the molecular level. In particular, on the basis of our experimental results, we found that the  $O(^3P, ^1D)$  + cyanoacetylene reaction leads to the following reactive product channels: OCCCN + H (BF = 0.10),  $^3HCCN/^1HCCN + CO$  (BF = 0.32), and  $^1HCCN + CO$  (BF = 0.58), the latter deriving directly from the reaction of  $O(^1D)$  present in the beam. Regarding the experiment on the  $O(^3P, ^1D)$  + acrylonitrile reaction, we have proved the presence of the H-elimination channel (H + HCOCHCN), with a BF of 0.09, and the CO-formation channel ( $CO + H_2CCNH$ ), with a BF of 0.91; both channels arise from the reactivity of  $O(^3P)$ , but the second one results from ISC to the singlet PES. It is noteworthy that, in the case of  $O(^3P, ^1D)$  +  $CH_2CHCN$ , we do not observe the expected very fast  $H_2CCNH/CH_2CN$  products from the  $O(^1D)$  reaction, which in contrast was clearly seen in the  $O(^3P, ^1D)$  + CHCCN reaction for the  $^1HCCN$  product: the presence of an entrance potential energy barrier in the triplet PES of the  $O(^3P)$  + CHCCN system decreases the reactivity of  $O(^3P)$ , allowing the emergence of the contribution of  $O(^1D)$ .

For both systems, a more detailed theoretical analysis, still underway, will determine the extent of the ISC from triplet to singlet PES and will provide statistical estimates of the product branching fractions for comparison with our experiment and for validation of the calculated PES. Once validated, the developed PES could be used to generate channel specific rate constants as a function of temperature and pressure, which are the quantities needed for developing or improving combustion models.

## Acknowledgments:

This work was supported by Italian MUR and University of Perugia (Department of Excellence-2018-2022-Project AMIS). P.L. and E.V.F.D.A. acknowledge support from the Marie Skłodowska-Curie project "Astro-Chemical Origins" (grant agreement No 811312). D.M. and F.F. acknowledge support from ASI (DC-VUM-2017-034, Grant n° 2019-3 U.O. Life in Space).

## References:

- [1] B. J. Finlayson-Pitts and J. N. Jr Pitts, *Atmospheric Chemistry – Fundamentals and Experimental Techniques* (Wiley, New York, 1986).
- [2] J. -F. Lamarque et al., *J. Geophys. Res.* **101**, 22955 (1996).
- [3] D. S. Lee et al., *Atmos. Environ.* **31**, 1735 (1997).
- [4] S. Wallace, K. D. Bartle, and D. L. Perry, *Fuel* **68**, 1450 (1989).
- [5] J. A. Miller and C. T. Bowman, *Prog. Energy Combust. Sci.* **15**, 287 (1989) and references therein.
- [6] N. R. Hore and D. K. Russell, *J. Chem. Soc., Perkin Trans. 2*, 269 (1998).
- [7] A. Terentis, A. Doughty, and J. C. Mackie, *J. Phys. Chem.* **96**, 10334 (1992).
- [8] A. Lifshitz, C. Tamburu, and A. Susulnsky, *J. Phys. Chem.* **93**, 5802 (1989).
- [9] E. Ikeda and J. C. Mackie, *Twenty-Sixth Symposium (International) on Combustion, The Combustion Institute*, 597 (1996).
- [10] H. Pan et al., *Chem. Soc. Rev.* **46**, 7517 (2017).
- [11] P. Casavecchia et al., *Phys. Chem. Chem. Phys.* **11**, 46 (2009).
- [12] A. M. Schmoltner, P. M. Chu, and Y. T. Lee, *J. Chem. Phys.* **91**, 5365 (1989).